IEEE Access
Multidisciplinary | Rapid Review | Open Access Journal

Received June 22, 2020, accepted July 2, 2020, date of publication July 13, 2020, date of current version July 23, 2020.

Digital Object Identifier 10.1109/ACCESS.2020.3008934

Low-Cost Microwave Components' Fabrication in Hybrid Technology of Laminates and Additive Manufacturing on an Example of Miniaturized Suspended Directional Coupler

JAKUB SOROCKI, (Member, IEEE), AND ILONA PIEKARZ, (Member, IEEE)
Electronics Department, AGH University of Science and Technology, 30-059 Kraków, Poland

Corresponding author: Jakub Sorocki (jakub.sorocki@agh.edu.pl)

This work was supported by the National Science Centre, Poland, under Grant 2019/34/E/ST7/00342. The work of Jakub Sorocki was supported by the Foundation for Polish Science (FNP) under Stipend START 080.2020.

ABSTRACT A low-cost approach for the fabrication of low-loss microwave components in hybrid technology of laminates and additive manufacturing is presented in this paper. A standard copper-cladded printed circuit board technology is used in combination with a basic stereolithographic 3D printing technology and industry-standard physical vapor deposition technology of aluminum for manufacturing one of the basic building blocks of microwave systems – a 3-dB coupled-line directional coupler in suspended technique operating at 2.0 GHz band. A thin laminate with the coupler traces' mosaic is suspended inside a metal-coated 3D printed enclosure. The presented study explores the performance of the circuit in terms of total power loss vs. the properties of deposited metallization layer serving as a ground plane. It is shown that when the surface roughness of the 3D printed enclosure is low enough, which can be achieved with the use of a layer of lacquer primer before metal deposition, the conductor-related power losses are lowered to an acceptable level. An exemplary directional coupler was developed along with three variants of the enclosure and the reference one. The measurement results validate the potential of this hybrid technique to deliver fully valuable microwave components at a very low manufacturing cost.

INDEX TERMS 3D printing, additive manufacturing, aluminium metallization, directional coupler, hybrid manufacturing technology, packaging microwave components, physical vapor deposition, stereolithography.

I. INTRODUCTION

Additive Manufacturing (AM) technologies have gained recently momentum due to increased interest for academic research as well as in industrial solutions since they respond to the expectations of today's needs such as the low-cost realization of complicated 3D geometries, ease of adjustment for mass production as well as minimum resource wastage [1]–[4]. Thus, the AM technologies, initially adopted for rapid prototyping to test the design before the final product development, rapidly evolved toward the complete (one-pass) manufacturing of end-use components [5], [6]. Significant development of the manufacturing equipment as well as material engineering has led to the availability of many 3D printing techniques, among which the most popular ones are FDM (fuse deposition modeling) and SLA (stereolithography) due to the wide access to the commercially available low-cost desktop printers.

Recently, radiofrequency (RF) engineers have started to leverage AM technologies, including 3D printing, to develop the next generation of microwave and millimeter-wave devices, among which are millimeter-wave wireless and satellite communication systems and *components* such as waveguides, sensors, antennas, filters, power dividers, etc. References [7]–[12]. While the realization of complex 3-D geometries out of dielectric materials is already well established, it can be observed, that it is still challenging to realize low-loss (low resistivity) conductive structures using 3-D printing technology, which is required for many RF devices. Importantly, at microwave frequencies, the current flows through the conductors only within a skin depth thick cross-section ranging between a few micrometers to hundreds

The associate editor coordinating the review of this manuscript and approving it for publication was Andrei Muller.

of nanometers. The above in combination with the conductor surface roughness contributes to the effective conductor resistivity that can be much higher than the one for bulk metal. Therefore, a variety of methods have been tested to address this issue. One of the methods is to use a special sputtering system, which allows covering the dielectric printed part with copper metal [7], [10]. This method yields very good results in terms of conductivity as hundreds of micron thick layer of copper can be deposited, however, requires a multi-step process to achieve good adhesion to a plastic surface and the sample can heat up to a point of permanent deformation due to the use of plasma in the process [13]. Another method described in the literature is the utilization of conductive filaments and the FDM-type 3D printing technique [14], [15], to print the conductive traces or surfaces that significantly simplifies the circuit manufacturing process. Nevertheless, to date, the available off-the-shelf filaments on the market provide insufficient for practical use conductivity, and therefore, additional processes such as electrodeposition of copper are needed on top [16]. Recently, the development works are conducted towards novel manufacturing technologies for printing the conductive parts out of metal powder through e.g. selective laser melting [17]. As of now, however, those processes are expensive, especially when the fine resolution for the realization of complex conductive geometry is required.

One of the most popular techniques of plastic metallization widely used in industry is the physical vapor deposition (PVD) method [18]. This coating technique is used in the automotive industry, packaging industry, for optical components, reflectors, etc. with its advantage being the coating time. With most metallic materials, the coating deposition needs only a few minutes once the required vacuum level is achieved as thicknesses of tens of nanometers are sufficient. Since the vapor-phase atoms condense on the relatively cold exposed surface of the plastic part, and thus, part heating is so slight that even highly temperature-sensitive materials maintain their shapes. The commonly used coating metal is aluminum due to its silvery brilliance and high adherence. Although the PVD technology is low-cost and utilized in mass production, its utilization in additively manufactured RF electronics has not been comprehensively studied so far.

In this paper, a detailed study on the usability of the vacuum metallization technique of the 3D printed parts is presented towards the low-cost fabrication of low-loss microwave systems using the hybrid technology of laminates and additive manufacturing. A standard copper-cladded printed circuit board technology is used in combination with basic masked stereolithography (MSLA) 3D printing technology and industry-standard physical vapor deposition of aluminum for manufacturing one of the basic building blocks of microwave systems – a 3-dB coupled-line directional coupler operating at 2.0 GHz band. The study explores the performance of the circuit in terms of total power loss vs. the conductivity of the deposited metallization layer serving as the circuit's ground plane on top of a 3D printed enclosure. Such fabrication is especially useful for the realization of low-loss circuits in suspended dielectric structures where dielectric-related losses are drastically reduced due to the introduction of lossless air filling. As a result, the conductor-related losses are the main loss mechanism, and thus, low effective resistivity metal of both the circuit traces and ground planes is of importance. To minimize the affection of dielectric related losses onto total power losses, the exemplary coupler circuit was realized in a suspended stripline technique exploring the enhanced 2.5D dielectric structure described in [19] where a thin center laminate with the coupler traces' mosaic is suspended over a locally variable air-layer thickness improving the coupler's performance. Additionally, the coupler was miniaturized through the quasi-lumped technique. The exemplary directional coupler was developed along with three variants of the enclosure and the reference one. The measurement results have shown that when the 3D printed enclosure surface roughness is small, the power losses are lowered to an acceptable level. When the printing technology does not deliver a given surface smoothness, a layer of lacquer primer can be used before metal deposition. The obtained results validate the potential of this hybrid technique to deliver fully valuable microwave components at very low manufacturing cost featuring reliable mechanical construction and relatively high electrical performance with low power losses.

II. MATERIALS AND METHODS

A. MINIATURIZED COUPLED-LINE DIRECTIONAL COUPLER DESIGN

A coupled-line directional coupler is a four-port device composed of two sections of a transmission line close to each other that enable some of the power delivered to the input port of one strip to be coupled through an electromagnetic coupling to the other strip's coupled port while the remaining power is transmitted to the first strip's transmitted port with the last port isolated. Coupled-line couplers feature wider operational bandwidth due to the above-described coupling mechanism in comparison to directly connected directional couplers, and therefore, are widely utilized in RF signal distribution networks. Applications such as power division and combination networks, power level monitoring circuits, measurement multi-ports, antenna feeding, and beam-forming networks [20] are some of the examples. The radio frequencies reserved internationally for industrial, scientific, and medical (ISM) purposes are allocated among other bands, also at lower frequencies up to 5.8 GHz, at which the coupled-line couplers occupy a relatively large area. Therefore, many techniques have been developed during the past years [21]–[23] allowing for couplers' size reduction. One of them [22], [23] is the quasi-lumped approach, where the coupled-line section is divided into n subsection and each of them is approximated through high-impedance coupled sections and lumped capacitors to realize the required per-unit-length inductive and capacitive elements. The miniaturization factor in this case depends on the maximum available coupling of the utilized dielectric structure. On the other

hand, there are a few techniques for the dielectric stack-up realization to choose from. One of them is the suspended stripline technique [19], [22] that have advantages such as symmetry of the dielectric structure and lower dielectric-related insertion losses as the center laminate is suspended over the upper and lower ground planes in-between two lossless air-filled layers. From the perspective of this study, the additional benefit is that the conductor-related losses make up the majority of the total power losses what is the main object of interest. The main disadvantage of the suspended stripline is the non-homogeneity of the medium (permittivity of air and permittivity of suspended laminate are different), which leads to coupler's performance deterioration when capacitive and inductive coupling coefficients equalization technique of the constitutive coupled-line section is not applied [24], [25]. On top of that, a robust enclosure is needed to serve both mechanical functions ensuring the integrity of the self-enclosed device and provision of proper suspension of the laminate with the coupler's mosaic over the air layers above the ground plane as well as the electrical function of provision of the uniform low-resistivity metal ground plane for the circuit where upper and lower surfaces are connected all together with ones on the laminate (if any). Recently, it has been shown that the development in additive manufacturing (3D printing and surface metallization) enables the realization of a lightweight conductive enclosure with features such as a locally variable air-layer thickness, giving the possibility to entirely or partially realize the coupler's compensating elements to improve its electrical performance [19].

In this study, a 3-dB (equal power split) coupled-line directional coupler was designed to operate at the center frequency of $f_0 = 2$ GHz. The approach shown in [19] was followed taking advantage of the enhanced 2.5D dielectric structure (as enabled by the fabrication technology) accompanied by the quasi-lumped element miniaturization technique described in [22] and performance improvement technique due to inhomogeneous medium [25]. An overcoupling of 0.6 dB @ f_0 is assumed as to obtain a coupling bandwidth. A stripline dielectric structure represented in Fig. 1 was used. A thin DuPont Kapton laminate of $h_{lam} = 50$ μm thickness and permittivity of $\varepsilon_{rlam} = 3.4$ (loss tangent $tan\delta_{lam} \approx 0.003$) providing metal layers $m1$ and $m2$ with 17 μm of copper was

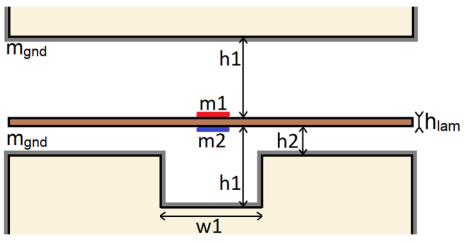

FIGURE 1. A cross-section view of the 2.5D enhanced stripline dielectric structure used for the design of a miniaturized coupler. A thin center laminate with two-sided metallization of m_1 and m_2 is suspended over the top and bottom ground planes m_{gnd} creating a thick lossless air layer. Width w_1 was selected in a way not to affect the coupled-line section.

suspended over the top and bottom ground planes m_{gnd} with $h_1 = 5$ mm layer of air in the coupled-line section region. The initial coupled-line strips' width w was chosen to be as narrow as possible (limited by the PCB fabrication tolerances here) to maximize the circuit miniaturization [22] and realize the required self-inductance L_1, thus $w = 0.12$ mm was set. Next, the required strips' mutual- and self- capacitances C_m and C_1, respectively were calculated for a maximum coupling available in the structure ($k_{max} = 0.893$) and the desired nominal coupling assuming that the coupler is divided into $n = 4$ subsections. The coupled-section's layout was further miniaturized by meandering the coupled strips. When designed properly as shown in [23] this has the additional advantage of partial realization of the C_1 and C_m capacitances, and thus reducing the remaining required lumped capacitances' footprint. On top of that, the ground plane was introduced on metals $m1$ and $m2$ as well for further reduction of C_1 footprint (as it is inversely proportional to the distance to the ground). Finally, the coupler's connecting signal transmission lines were designed with the air-layer underneath altered to an optimized thickness of $h_2 = 0.3$ mm (see Fig. 2) to reduce the footprint of transition region compensating capacitance and decrease the lines' width as presented in [19] for better circuit compactness.

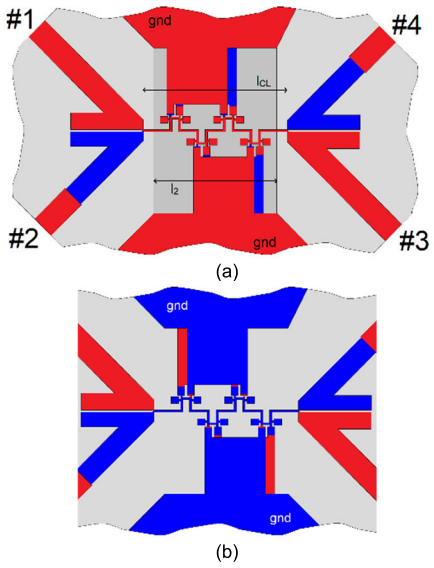

FIGURE 2. Top (a) and bottom (b) view of the designed coupler's layout. Top metal m_1 is depicted in red while bottom metal m_2 in blue; the region of h_1 air layer underneath the miniaturized coupled-line section is depicted in dark gray. The functional port notation is assumed here as: #1 is the input port, #2 is the coupled port, #3 is the thru port and #4 is the isolated port. However, the functionality is maintained with proper relation when either of the ports is selected as input. Coupler's length over the thick air layer is $l_2 = 7.98$ mm while the total length of the coupled-line section is $l_{CL} = 9.26$ mm.

The final layout of the developed miniaturized 3-dB coupler is presented in Fig. 2 while the frequency response calculated through the full-wave electromagnetic (EM) simulation (coupler and connecting lines) using NI AWR Design Environment software with AXIEM 2.5D solver is provided

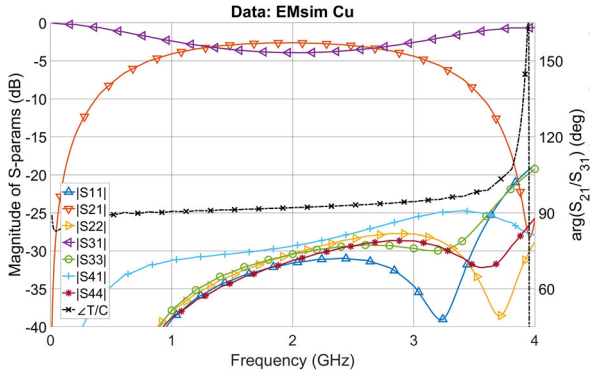

FIGURE 3. EM simulated frequency characteristics of the designed coupler as for the layout shown in Fig. 2 that include the coupled-line section, compensated transitions, and 12 mm long sections of transmission lines.

in Fig. 3. As seen, the coupler features equal power split with an imbalance of $\delta_C \approx \pm 0.6$ dB and coupling bandwidth of ∼2.6, a quadrature-phase difference between coupled and through ports, and isolation/impedance match better than −35 dB within the operational bandwidth. Total power loss calculated for perfectly smooth, 17.5 μm thick copper metal on $m1$, $m2$, and lower/upper ground planes equals 0.20 dB @ f_0 (0.11 dB for the miniaturized coupled-line section only). It needs to be underlined, the coupler's layout is two times smaller as compared to a classic coupled-line coupler realized in a homogeneous dielectric structure of permittivity $\varepsilon_r = 3.4$.

B. CIRCUIT'S FABRICATION

The fabrication process of the designed circuit for the experimental study was done in three steps i.e., i) fabrication of coupler's mosaic on the laminate through PCB technology, ii) additive manufacturing of multiple identical units of the enclosure through the 3D printing technology, iii) metallization of the enclosures through the PVD technology with varied process parameters. All of the above can be done at a very low-cost, especially for high volume production. The same pre-assembled laminate inset was used in combination with all the enclosures to reduce the number of variables affecting the coupler's performance down to the ground plane metallization only.

1) COUPLER'S CENTER LAMINATE FABRICATION THROUGH THE PCB TECHNOLOGY

For circuit fabrication, the manufacturing version of the layout was prepared. For ease of assembly and integration of PCB with the enclosure, a transition from m_2 to m_1 was added to the connecting transmission lines to make all the ports to be on the same top (as referenced to the ground plane below m_2) metal layer. Moreover, to allow for a reliable ground plane connection between the SMA connector and couplers' enclosure, the ground planes on m_1/m_2 were extended to the PCB's edges mating with the connectors' ground. Such a configuration allows for pre-assembly of the PCB reducing the number of assembly failure points since both center pin as well as outer conductor of the SMA connectors can be directly soldered to the coupler's metal on the laminate. Otherwise, those grounds could not be connected, as soldering to the aluminum metalized enclosure is hardly possible. Moreover, indentations were added to limit the solder flow beyond the connector sides so the solder is restrained and does not interfere with the enclosure walls when assembled. To ensure proper connection between the ground planes on the laminate and the metalized surface of the 3D enclosure, a metal skirt around the circuit on the $m1$ and $m2$ metal layers was added creating a large surface area for pressure contact.

The PCB was manufactured using the photolithography method where a masking film with the circuit pattern is used to expose a UV-light sensitive photoresist layer that the bare laminate is coated with beforehand. Then, the unwanted metal is etched down (chemical etching with sodium persulfate as the etchant solution) leaving the circuit traces. A photograph of the unit is shown in Fig. 4.

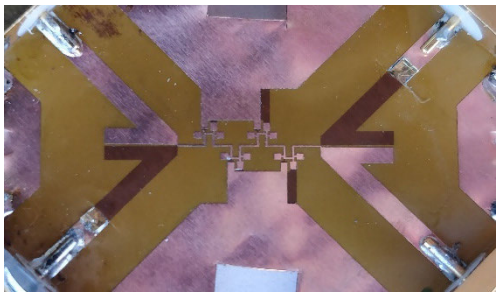

FIGURE 4. Photograph of the in-house fabricated PCB (chemical etching, sodium persulfate as the etchant solution) on a thin laminate with the designed coupler traces and four SMA connectors soldered visible.

2) COUPLER'S ENCLOSURE FABRICATION THROUGH THE M-SLA 3D PRINTING TECHNOLOGY

For fabrication, the manufacturing version of the enclosure was designed using a 3D modeling CAD software based on the primitives exported out of the EM CAD software. The final model of the enclosure was created considering the up-and-down sides of manufacturing through the 3D printing process and the final assembly of the hybrid circuit. The two-piece enclosure together with the inner laminate is intended to comprise a self-enclosed circuit. For that reason, the mechanical and electrical features are complementary to each other. To ensure mechanical strength and mounting points for the top and bottom halves of the enclosure as well as to provide a low-inductance connection between top and bottom ground planes, large surface area pads were designed together with a set of lego-like tightly-fitted post and hole elements. Moreover, brackets for SMA connectors were added to allow for the reduction of peeling force on the laminate while coaxial cables are connected during measurements.

The enclosure was manufactured using the *Prusa Research* hardware-software ecosystem for hobbyists. The Original Prusa SL1 printer was used, which is an M-SLA printer utilizing a high-resolution LCD panel having a pixel size of 47 μm and a UV LED panel to cure thin layers of resin.

A high-quality UV photosensitive transparent tough liquid was chosen as a base material. The CAD software exported model was sliced using the Prusa Slic3r software at 0.1 mm layer height being aligned with an integer multiple to the minimum step in the Z-axis of the model (here 0.3 mm) to generate the printer commands file. The default curing profile for the tough resin was used. Models parts were placed directly on the build platform to ensure maximally flat and even X-Y surfaces which are crucial for achieving good effective conductivity of the ground plane. This way the surface of the finished print is only affected by the size and construction of the LCD. The UV light during the curing process is being shuttered by the pixel edges resulting in uneven exposure of the resin and thus peaks and valleys reflecting the panel arrangement. Supports were added only in the region of the SMA holders. The printed units were post-processed by cleaning and curing them using the Original Prusa CM1 curing-washing machine. The photograph of an exemplary unit of the 3-D printed enclosure is presented in Fig. 5.

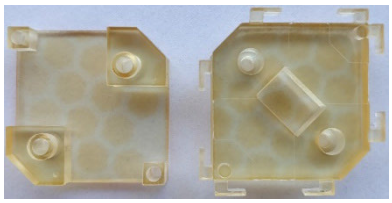

FIGURE 5. Photographs presenting the in-house 3D printed enclosure that after metalizing will host the coupler's thin center laminate. The outer dimensions after assembly are 30.5 mm x 30.5 mm x 14 mm.

3) COUPLER'S ENCLOSURE METALLIZATION THROUGH THE PVD TECHNOLOGY

Since the main function of the printed enclosure is not only the mechanical support for the suspended thin laminate with the coupled-line coupler mosaic but also ensuring ground plane for the circuit, the 3-D printed part was in the next step metalized. For this purpose, one of the most popular techniques, widely used in industry for mass-production i.e., the PVD method was utilized. The enclosure was metalized by a local company, that provides services of metallization and processing of plastics in a majority for automotive reflectors and cosmetic packages. Process settings of a metal coating run and machinery used is the company's know-how and is outside of the scope of this study. A common practice in those cases is to put a layer of lacquer before metal deposition for improved reflectiveness of the surface as the treatment reduces plastic surface roughness by filling all the unevenness. The same pre-processing can be beneficial for microwave circuits as the effective metal resistivity increases with roughness. Therefore, three variants of the enclosure were manufactured and tested with altered process parameters, namely A1-A3 were:

a) A1 (L1A2) uses a 3 step process: the raw part coated with one layer of lacquer primer → first run of thin aluminum layer deposition onto the part in the vacuum chamber → second run of thin aluminum layer deposition onto the part in the vacuum chamber;
b) A2 (L0A2) uses a 2 step process: first run of thin aluminum layer deposition onto the raw part in the vacuum chamber → second run of thin aluminum layer deposition onto the part in the vacuum chamber;
c) A3 (L2A1) uses a 3 step process: raw part coated with first layer of lacquer primer → part coated with the second layer of lacquer primer → one run of thin aluminum layer deposition onto the part in the vacuum chamber;

Moreover, an extra reference enclosure was manufactured, namely C4 where:

d) C4 (L0C1) uses a 1 step process: the raw part is taped with a 25 μm thick copper tape with adhesive backing.

Photographs of the metalized 3-D printed enclosures A1-A3, C4 are shown in Fig. 6.

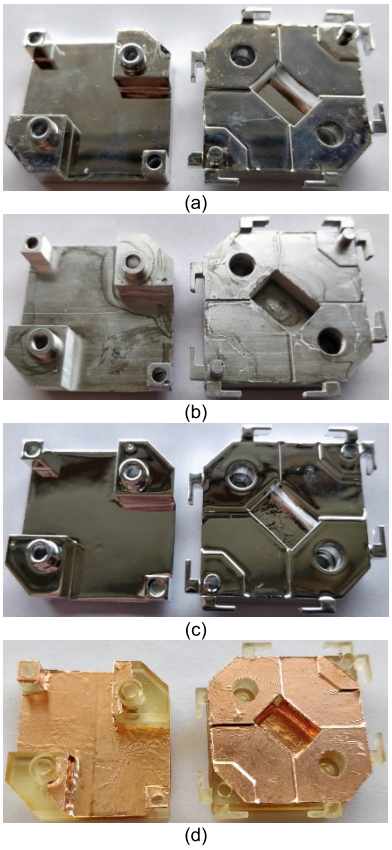

FIGURE 6. Photographs of the external company metalized two-part enclosure for the designed directional coupler in four different variants: A1 – one coat of lacquer, two runs of aluminum deposition (a), A2 - no lacquer, two runs of aluminum deposition (b), A3 - two coats of lacquer, two runs of aluminum deposition (c) and C4 – no lacquer, copper taped (d). The part reflectiveness is mainly affected by its surface roughness.

4) COUPLER'S ASSEMBLY

After manufacturing all the parts, the coupler circuit was assembled. At first, the laminate was pre-assembled by soldering all four SMA connectors to the m_1 metal. After that,

two halves of the enclosure were snapped together with the laminate in the middle using the lego-like process. A set of screws was used to tighten all the press-contact regions of ground planes on the enclosure and laminate into one unified, galvanically connected ground plane. Photographs presenting the fully assembled, self-enclosed component are shown in Fig. 7.

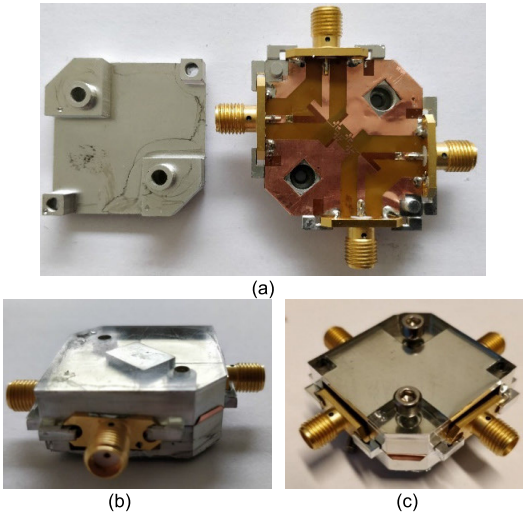

FIGURE 7. Photographs presenting the assembly process of the developed coupled-line coupler: the thin laminate with pre-soldered connectors is fitted into the bottom part of the assembly (a), the top and bottom sub-enclosures are snapped together with the laminate in the middle (b) and screws are added for better press-contact of ground planes (c).

III. RESULTS

The usability of the proposed low-cost hybrid manufacturing approach towards the realization of microwave components was evaluated based on the measurement results of the developed samples that share the same circuit design. The end-goal here is to verify if the effective resistivity of the additively manufactured enclosure's ground plane is low enough to yield total microwave power losses at an acceptable level for circuits operating in the frequency range of a few gigahertzes.

First of all, the scattering parameters of the manufactured directional coupler for four different variants of the ground plane (enclosure) metallization were measured. The *Agilent* PNA Network Analyzer N5227A calibrated using SOLT standards with the reference plane set at the SMA connectors plane was used. For each tested enclosure, the same manufactured center laminate piece was used since closely matched performance in each case is essential from the perspective of this study as in opposition to the absolute performance of the coupler. The measured S-parameters are displayed in Fig. 8 while parameters of interest are summarized in Table 1. The observable inter-variant difference is mainly due to three reasons:

- The laminate-to-ground distance of h_2 and h_3 differs what is especially pronounced for small thicknesses. As a result, the effective permittivity in the connecting line and transition compensation region varies, influencing the impedance match. E.g. reduction of h_3 by $\Delta h_3 = 50\ \mu$m leads to impedance match reduction by ~ 6 dB @ f_0.

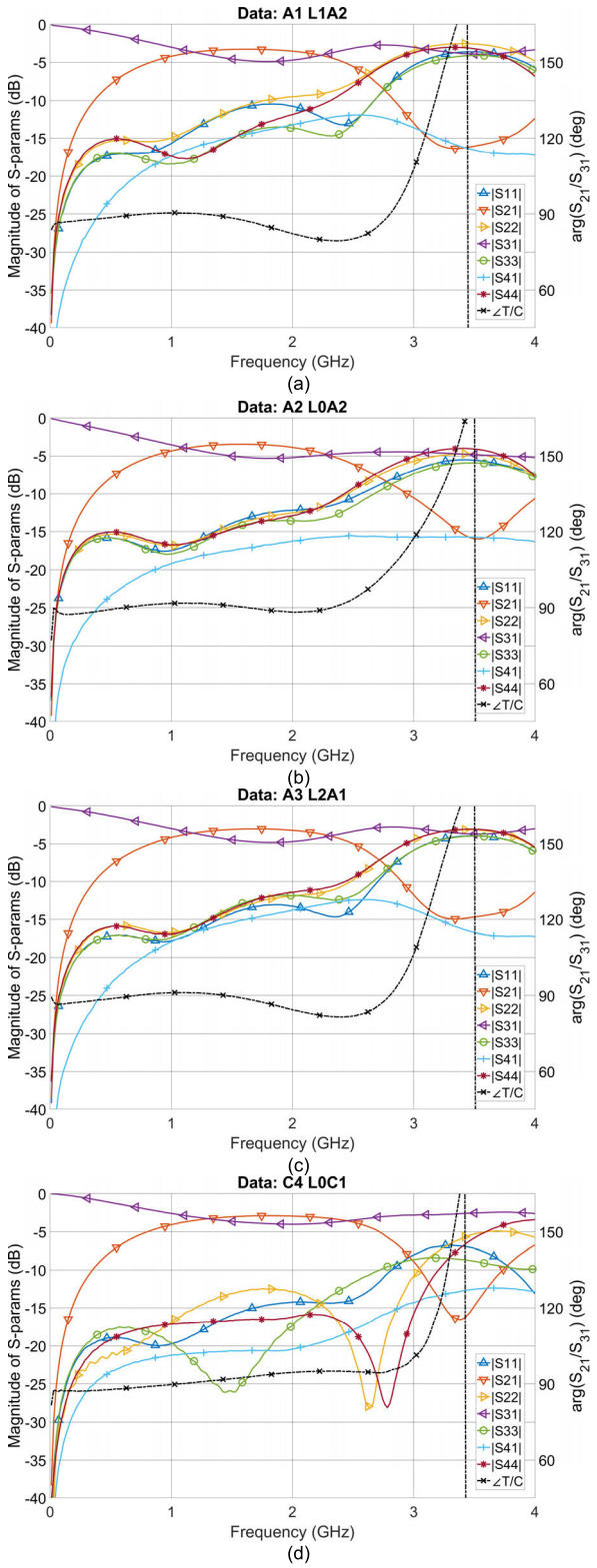

FIGURE 8. Measured S-parameters of the developed suspended directional coupler for four variants of the enclosure metallization variants: A1 (a), A2 (b), A3 (c), and reference C4 (d).

TABLE 1. Summary of the measured parameters of the manufactured directional coupler for each of the enclosure variant.

Coupler variant	center freq. f_0 (GHz)	coupling C |S21| @ f_0 (dB)	transmission T |S31| @ f_0 (dB)	phase diff arg(T/C) @ f_0 (deg)	port avg. tot. power loss @ f_0 (dB)
A1 (L1A2)	1.71	-3.29	-4.87	86.2	0.366
A2 (L0A2)	1.71	-3.48	-5.27	89.5	0.846
A3 (L2A1)	1.75	-3.04	-4.81	87.4	0.393
C4 (L0C1)	1.89	-2.89	-3.98	94.0	0.238
EM sim	2.00	-2.62	-3.92	92.1	0.202

- Since the used laminate is very thin and there is not much metal on it to stiffen the sheet, it can slightly flex leading to variation of laminate-to-ground distance. This might have happened even though the laminate/enclosure is assembled in a way to put a small and uniform tension on the laminate in a longitudinal direction to prevent this effect. The result is quite similar to the first case.
- Variation in length l_2 of the h_2 thick layer underneath the coupled-line section (as a result of 3D model reproduction with an accuracy of the pixel size (here $\pm$ 47/2 μm) and/or adding an extra layer (like lacquer) to the vertical wall of the printed enclosure) change the electrical length of the coupler and thus its center frequency of operation is shifted.
- Finite print-to-print tolerances and assembly accuracy affection.

Following, the total RF power loss within the circuit (directional coupler along with connecting transmission lines) was determined for each enclosure variant (as a difference between total power delivered to a given input port and powers transmitted to remaining ports and reflected from the input port) and is provided in Fig. 9. Importantly, even though the total loss is a sum of conductor losses and dielectric losses (which tend to increase with frequency) this does not affect the comparison results as the same dielectrics and $m_{1,2}$ metals are used. Therefore, it is safe to assume that the observed variation is due to differences in the ground plane metallization. It is seen that the reference C4 enclosure with 25 μm of copper provides the lowest power losses of 0.238 dB @ f_0, as it was expected. Moreover, the loss level matches the one determined from EM simulations where 0.5 Cu/oz was assumed (see Section II.A for reference). Interestingly, the A1 and A3 enclosure provides almost identical performance with total losses of 0.366 dB @ f_0 and 0.393 dB @ f_0, respectively. The A2 variant where no lacquer primer is used provides the highest losses of 0.846 dB @ f_0. This is more than a 1.1169-fold increase (linear scale for power) with respect to A1, even though the coated metal thickness is roughly the same. From the perspective of the microwave circuit realization, the already provided data can be used to draw initial conclusions:

- The strategy of A1 and A3 metallization yield better results of A2 for obtaining lower losses.

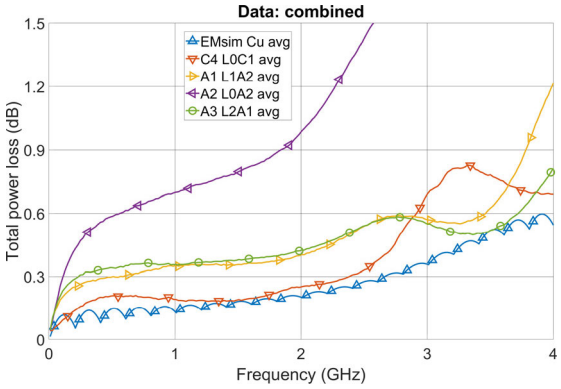

FIGURE 9. Averaged (across values derived for each port treated as the input one) total power losses calculated out of the measured S-parameters for enclosure variants: A1, A2, A3, and C4 of the directional coupler sharing the same manufactured center laminate along with the EM simulation reference data. The observed variation in losses is attributed to the difference in the ground plane properties.

- Even though the power losses of A1/A3 are 1.03-/1.036-fold higher than of C4, the strategy of A1/A3 is useful for manufacturing considering its very low cost.

However, the above does not paint the whole picture, and the strategy to minimize the total losses can be further identified. It needs to be noted first, that the total power loss is associated with effective properties of all the metal layers of the circuit which in this comparative study boils down to the difference in the ground plane properties. The effective resistance of the metal is a resultant of the bulk metal resistivity and its surface thickness and surface roughness. The above ingredients are bounded with the general relation:

$$R_{eff} = r\rho\frac{L}{A} = r\frac{\rho}{t_c}\frac{L}{W} = rR_{Sq}\frac{L}{W}(\Omega) \tag{1a}$$

$$\begin{cases} t_c = t \\ t_c = \delta = \sqrt{\dfrac{2\rho}{2\pi f \mu_0 \mu_r}} \end{cases} \quad for \begin{array}{l} t \le \delta \\ t > \delta \end{array} \tag{1b}$$

where R_{eff} is the effective metal resistance, ρ is bulk resistivity in (Ω/m), A is the sheet cross-section area which can be split into current flow thickness t_c (m) and width of W (m), t is the sheet thickness, δ is the current skin depth, L (m) is the sheet length parallel to which the current flows, R_{Sq} is the sheet resistance (Ω/sq) and r is a generalized surface roughness coefficient; f (Hz) is the frequency and $\mu_0\mu_r$ is the absolute permeability of the material. Therefore, the metal's effective sheet resistance (rR_{Sq}) was measured along with the surface profile for A1-A3 enclosures. As a point of reference for further considerations, the following information is useful. The bulk resistivity of copper equals ρ_{Cu} = 1.68e-8 @ 20°C while of aluminum equals ρ_{Al} = 2.65e-8 @ 20°C. The resulting current skin depth at the center frequency of the developed coupler for copper equals δ_{Cu} = 1.58 μm @ 1.7 GHz (0.29 μm @ 50 GHz) while for aluminum equals δ_{Al} = 1.99 μm @ 1.7 GHz (0.37 μm @ 50 GHz). Therefore, it is safe to assume $t_c = t$ for A1-A3 while $t_c = \delta$ for C4. In general, the skin depth value can be used to determine the

minimum metal thickness (determined for lowest frequency of operation) that ensures the effective resistivity of the layer equates the material's bulk one assuming a perfectly smooth surface.

The effective sheet resistance was measured using *Picotest* M3500A meter with four-terminal probe and the following results were obtained: $R_{sq\_A1} = 0.3805\ \Omega$/sq, $R_{sq\_A2} = 1.314\ \Omega$/sq, $R_{sq\_A3} = 0.725\ \Omega$/sq. Following, the relative surface profile was captured using the Taylor Hobson TalyStep profilometer and the digitized analog print-out data is provided in Fig. 10. From the data, the LCD-masking matrix arrangement can be clearly seen. A repeated pattern of hills and valleys with spacing matching the 47 μm pixel size. Moreover, for the A2 (L0A2) version, the resin unevenness of exposure due to non-100% light passing surface area of the pixel manifest through surface roughness of over 100 nm peak-to-valley. On the other hand, when the lacquer primer is used, as in A1 (L1A2), the surface roughness is reduced to roughly 5 nm peak-to-valley. Similar results are obtained for A3 (L2A1). Out of that, rearranging eq. 1, and under the assumption of conductivity being equal to one of bulk aluminum and neglecting the influence of surface roughness, the metal thickness can be estimated out of the measured effective sheet resistance to be in the range of 45-50 nm for A1 and in the range of 22-25 nm for A3.

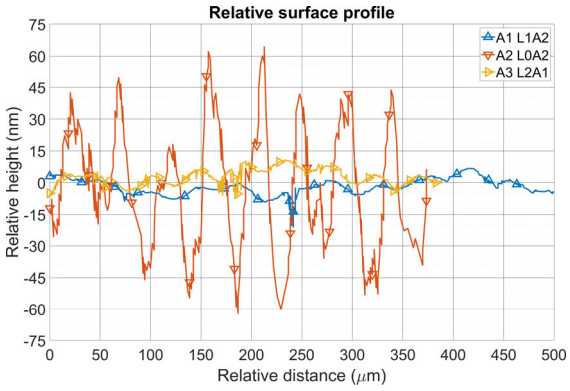

FIGURE 10. Measured relative surface profiles captured for the stylus paths aligned to the pixel grid arrangement of the used LCD-SLA printer for enclosure variants: A1, A2, and A3. The flat part of the top sub-assembly of the enclosure was cut-out and characterized.

The above-presented results cast more light on the usability of the proposed manufacturing approach and allow to draw further conclusions and requirements:

- It is seen that the surface roughness is the major factor for effective metal losses. This is especially important considering the metal layer itself deposited using PVD is rather thin compared to current skin depth.
- A high correlation between surface roughness pattern and the construction of the masking LCD of the SLA printer is observed. The peak-to-valley variation is the higher as the higher is the shadowing effect of pixel edges compared to the pixel center.
- Even one layer of lacquer primer, considering the used SLA technology' pre-processed surface roughness, before the metallization process provides a great improvement in the resulting metal resistance.
- For no-high-resolution demanding circuits, the SLA technology can be replaced with the FDM type what reduces costs and materials used and are well suitable for PVD metallization at the expense of using more coats of lacquer primer to smoothen the much rougher pre-process surface.
- Alternatively, when instead of LCD-SLA the DLP-SLA (Digital Light Processing) 3D printing technology is used, where instead of a fixed matrix of pixels, a laser scanning optics is used with continuous focused laser beam path, the pre-processed surface roughness should be reduced as little-to-no varied light intensity is observed, and therefore, no lacquer primer is needed. This is at the expense of higher costs of the DLP-SLA machines compared to LCD-SLA.
- No metal adhesion issues were observed for all enclosure variants.
- Even at mm-wave-length frequencies, the current skin depth does not go below hundreds of nanometers. Therefore, in the case of using PVD metallization, all the conductor related loss is attributed to the thin metal layer which is strongly impacted by the surface roughness. See A2 vs. A1 where a 20-fold rougher surface increases the effective sheet resistance by the factor of 3.45.
- There is a lower frequency limit of usability since the aluminum layer thickness is much lower than the skin depth down to which the current could flow resulting in the conductor resistivity at an unacceptable level.

In general, the obtained experimental results are very satisfactory and certify that the proposed low-cost hybrid manufacturing can be successfully applied for circuits and systems' realization operating within the microwave frequency range.

IV. DISCUSSION

In this study, we investigated the approach for low-cost fabrication of microwave systems with lowered power losses through a hybrid technology of laminates and additive manufacturing on an example of one of the basic building blocks – a coupled-line directional coupler. The exploited manufacturing technologies are well known and very low cost, starting from the industry-standard PCB manufacturing, through the hobbyist-grade M-SLA technology, and finally industry-standard PVD technology. The exemplary directional coupler was developed along with three variants of the enclosure with aluminum coating and the reference copper-coated one. The measurement results have shown that when the 3D printed enclosure surface roughness is small, the power losses are lowered to an acceptable level, here being only a 1.03-fold higher @ f_0 than for a standard thick copper ground plane.

Although only an exemplary coupled-line coupler was presented, the fabrication approach is well suited for the

realization of other passive microwave devices in suspended microstrip/stripline technique such as filters, feeding networks, antennas, etc. as well as it enables convenient integration with the active building blocks such as amplifiers, transceivers, etc. into larger sub-systems. The used combination of technologies for manufacturing not only enables the realization of low-loss components but also low weight and fabrication time accompanied by high design flexibility [26]. On top of that, a large area format available with multi-layer printed circuit boards (PCBs) is available. Finally, solutions such as integrated cooling of active parts [27] for efficiency improvement due to the use of 3D printing, or patterned metal layer when proper masking technique is used before PVD coating are possible as well.

The obtained results show, that the proposed approach allows for obtaining comparable total loss to the circuits described in the literature (see Table 2) realized using PCB and/or metal or printed enclosure.

TABLE 2. Features comparison of the proposed directional coupler with other suspended coupled-line couplers.

Reference	[28]	[29]	[19]	**This work, A3**
Coupler type	single-section 3dB coupler in stripline	single-section 3dB tandem in stripline	single-section 3dB coupler in suspended stripline	miniaturized single-section 3dB coupler in suspended stripline
Laminate	Two-sided PCB	Multilayer PCB	Two-sided PCB	Two-sided PCB
Enclosure	Machined stock, solid aluminum	-	Magnetron sputtered PolyJet 3D printed piece, single µm of copper	PVD coated M-SLA 3D printed piece – tens of nm of aluminum
Coupler area (mm^2)	N.A.	22.3 x 15.5	10.6 x 3.1	9.3 x 3.1
f_0 (GHz)	2.5	2.25	6	1.75
Ret. loss (dB)	> 26	> 20	> 15	> 10
Isolation (dB)	> 28	> 20	> 20	> 12
Phase diff.	N.A.	90.5 ± 2.5°	84.2° ± 1°	86° ± 4.3°.
Air layer vs max coupling	fixed height/ limited C_{max}	fixed height/ limited C_{max}	var. height/ unlimited C_{max}	var. height/ unlimited C_{max}
The total loss at f_0	0.1* dB 0.04 dB/GHz	0.45^{+} dB 0.2 dB/GHz	0.55$^{\#}$ dB 0.09 dB/GHz	0.4$^{\wedge}$ dB 0.23 dB/GHz

* includes the directional coupler and short connecting transmission lines
$^{\#}$ includes the directional coupler and long connecting transmission lines
$^{+}$ directional coupler only
$^{\wedge}$ includes directional coupler and 12 mm long connecting transmission lines, drops to 0.3 dB for 3 mm long lines.

The obtained results have proven, that the hybrid laminate - AM technology is disruptive and enabling technology for the realization of microwave devices, what is promising for the next generation of communication systems, where there will be a need for low-cost in high-volume production, lightweight systems with increased power efficiency. Nevertheless, there are still challenges for the use of this technique. At lower frequencies, such as sub-GHz LTE bands, the metallization thickness might be insufficient, however, the aluminum layer is a very good base for copper plating, which can be performed when lower total losses are of interest. Another challenge for the proposed approach is an issue with soldering to aluminum, which is hardly possible. This problem can be however solved by appropriate design of an assembly build-up based on tight-fitting and pressure contact, as it was shown in this paper or by plating a thin layer of copper. Finally, metal adhesion when components are exposed to mechanical stress or temperature variation needs to be evaluated as metal cracking or peeling causes a failure when a part is in use. If that would be a case, stresses could be reduced by the proper mechanical design of the assembly while a high heat resistant resin for 3D printing can be used to reduce the temperature deformation.

V. CONCLUSION

The hybrid fabrication of electronics was studied that utilizes both subtractive and additive manufacturing techniques. It was shown that microwave components can be successfully fabricated through a low-cost process when a specified step is followed and given requirements are met to delivered close or comparable performance to all-metal enclosure counterparts. The approach was validated on an example of one of the basic RF system building blocks – a coupled-line directional coupler operating in S-band. A suspended stripline technique was used as in such case the metal related losses are the main power loss mechanism. The manufactured unit was studied in terms of total power loss vs. 3D print surface treatment and metal coating processing and compared with a reference circuit. The approach was confirmed to be of practical use.

ACKNOWLEDGMENT

The authors wish to thank the company Stanisz - Przetworstwo *i* Metalizacja Tworzyw Sztucznych, Gdow, Poland, for aluminum coating of the 3D printed parts and Jerzy Sokulski, Department of Electronics, AGH UST for measuring the surface profiles of enclosures.

REFERENCES

[1] B. Berman, "3-D printing: The new industrial revolution," *Bus. Horizons*, vol. 55, no. 2, pp. 155–162, Mar. 2012.
[2] E. MaCdonald, R. Salas, D. Espalin, M. Perez, E. Aguilera, D. Muse, and R. B. Wicker, "3D printing for the rapid prototyping of structural electronics," *IEEE Access*, vol. 2, pp. 234–242, 2014.
[3] I. Gibson, D. Rosen, and B. Stucker, *Additive Manufacturing Technologies 3D Printing, Rapid Prototyping, and Direct Digital Manufacturing*, 2nd ed. New York, NY, USA: Springer, 2015.
[4] B. Zhang, Y.-X. Guo, H. Zirath, and Y. P. Zhang, "Investigation on 3-D-printing technologies for millimeter-wave and terahertz applications," *Proc. IEEE*, vol. 105, no. 4, pp. 723–736, Apr. 2017.
[5] S. A. Nauroze, J. G. Hester, B. K. Tehrani, W. Su, J. Bito, R. Bahr, J. Kimionis, and M. M. Tentzeris, "Additively manufactured RF components and modules: Toward empowering the birth of cost-efficient dense and ubiquitous IoT implementations," *Proc. IEEE*, vol. 105, no. 4, pp. 702–722, Apr. 2017.

[6] R. Sorrentino and O. A. Peverini, "Additive manufacturing: A key enabling technology for next-generation microwave and millimeter-wave systems [point of view]," *Proc. IEEE*, vol. 104, no. 7, pp. 1362–1366, Jul. 2016.
[7] J. A. Byford, M. I. M. Ghazali, S. Karuppuswami, B. L. Wright, and P. Chahal, "Demonstration of RF and microwave passive circuits through 3-D printing and selective metalization," *IEEE Trans. Compon., Packag., Manuf. Technol.*, vol. 7, no. 3, pp. 463–471, Mar. 2017.
[8] J. Teniente, J. C. Iriarte, R. Caballero, D. Valcazar, M. Goni, and A. Martinez, "3-D printed horn antennas and components performance for space and telecommunications," *IEEE Antennas Wireless Propag. Lett.*, vol. 17, no. 11, pp. 2070–2074, Nov. 2018.
[9] V. Bharambe, D. P. Parekh, C. Ladd, K. Moussa, M. D. Dickey, and J. J. Adams, "Vacuum-filling of liquid metals for 3D printed RF antennas," *Additive Manuf.*, vol. 18, pp. 221–227, Dec. 2017.
[10] M. I. Mohd Ghazali, S. Karuppuswami, A. Kaur, and P. Chahal, "3D printed high functional density packaging compatible out-of-plane antennas," *Additive Manuf.*, vol. 30, Dec. 2019, Art. no. 100863.
[11] W. Clower, M. J. Hartmann, J. B. Joffrion, and C. G. Wilson, "Additive manufactured graphene composite sierpinski gasket tetrahedral antenna for wideband multi-frequency applications," *Additive Manuf.*, vol. 32, Mar. 2020, Art. no. 101024.
[12] J. Sorocki, I. Piekarz, K. Wincza, S. Gruszczynski, and J. Papapolymerou, "Broadband microwave microfluidic coupled-line sensor with 3-D-printed channel for industrial applications," *IEEE Trans. Microw. Theory Techn.*, vol. 68, no. 7, pp. 2808–2822, Jul. 2020.
[13] J. Sorocki, I. Piekarz, S. Gruszczynski, K. Wincza, and J. Papapolymerou, "Application of additive manufacturing technologies for realization of multilayer microstrip directional filter," in *Proc. IEEE 68th Electron. Compon. Technol. Conf. (ECTC)*, San Diego, CA, USA, May 2018, pp. 2470–2476.
[14] J. Sorocki, S. Koryciak, I. Piekarz, S. Gruszczynski, and K. Wincza, "Investigation on additive manufacturing with conductive PLA filament for realisation of low-loss suspended microstrip microwave circuits," in *Proc. Int. Conf. Electr., Electron. Syst. Eng. (ICEESE)*, Kanazawa, Japan, Nov. 2017, pp. 48–51.
[15] I. Piekarz, J. Sorocki, K. Wincza, S. Gruszczynski, and J. Papapolymerou, "Suspended microstrip low-pass filter realized using FDM type 3D printing with conductive copper-based filament," in *Proc. IEEE 68th Electron. Compon. Technol. Conf. (ECTC)*, San Diego, CA, USA, May 2018, pp. 2470–2476.
[16] M. J. Kim, M. A. Cruz, S. Ye, A. L. Gray, G. L. Smith, N. Lazarus, C. J. Walker, H. H. Sigmarsson, and B. J. Wiley, "One-step electrodeposition of copper on conductive 3D printed objects," *Addit. Manuf.*, vol. 27, pp. 318–326, May 2019.
[17] P. A. Pidge and H. Kumar, "Additive manufacturing: A review on 3D printing of metals and study of residual stress, buckling load capacity of strut members," *Mater. Today, Proc.*, vol. 21, pp. 1689–1694, 2020.
[18] W. Bialojan and M. Geisler, "Vacuum metallizing plastic parts," *Focus, Plating Plastics*, vol. 10, pp. 46–52, Oct. 1992.
[19] J. Sorocki, I. Piekarz, S. Gruszczynski, K. Wincza, and J. Papapolymerou, "Application of 3-D printing technology for the realization of high-performance directional couplers in suspended stripline technique," *IEEE Trans. Compon., Packag., Manuf. Technol.*, vol. 9, no. 8, pp. 1652–1658, Aug. 2019.
[20] D. Pozar, *Microwave Engineering*. New York, NY, USA: Wiley, 2005.
[21] S. Rehnmark, "Meander-folded coupled lines," *IEEE Trans. Microw. Theory Techn.*, vol. MTT-26, no. 4, pp. 225–230, Apr. 1978.
[22] K. Wincza and S. Gruszczynski, "Miniaturized quasi-lumped coupled-line single-section and multisection directional couplers," *IEEE Trans. Microw. Theory Techn.*, vol. 58, no. 11, pp. 2924–2931, Nov. 2010.
[23] I. Piekarz, J. Sorocki, K. Wincza, and S. Gruszczynski, "Modeling and performance improvement of folded coupled lines in miniaturized quasi-lumped directional couplers," *Int. J. RF Microw. Comput.-Aided Eng.*, vol. 25, no. 1, pp. 1–9, Jan. 2015.
[24] K. Sachse, "The scattering parameters and directional coupler analysis of characteristically terminated asymmetric coupled transmission lines in an inhomogeneous medium," *IEEE Trans. Microw. Theory Techn.*, vol. 38, no. 4, pp. 417–425, Apr. 1990.
[25] S. Gruszczynski and K. Wincza, "Generalized methods for the design of quasi-ideal symmetric and asymmetric coupled-line sections and directional couplers," *IEEE Trans. Microw. Theory Techn.*, vol. 59, no. 7, pp. 1709–1718, Jul. 2011.
[26] R. Bahr, B. Tehrani, and M. M. Tentzeris, "Exploring 3-D printing for new applications: Novel inkjet-and 3-D-printed millimeter-wave components, interconnects, and systems," *IEEE Microw. Mag.*, vol. 19, no. 1, pp. 57–66, Jan. 2018.
[27] M. Craton, M. I. M. Ghazali, B. Wright, K. Y. Park, P. Chahal, and J. Papapolymerou, "3D printed integrated microfluidic cooling for high power RF applications," in *Proc. Int. Symp. Microelectron.*, vol. 2017, no. 1, pp. 000675–000680, 2017.
[28] K. Wincza and S. Gruszczynski, "Method for the design of low-loss suspended stripline directional couplers with equalized inductive and capacitive coupling coefficients," *Microw. Opt. Technol. Lett.*, vol. 51, no. 2, pp. 315–319, Feb. 2009.
[29] Y. Wang, K. Ma, and S. Mou, "A high performance tandem coupler using substrate integrated suspended line technology," *IEEE Microw. Wireless Compon. Lett.*, vol. 26, no. 5, pp. 328–330, May 2016.